Mon. Not. R. Astron. Soc. **000**, 1–6 () Printed 21 June 2024 (MN LATEX style file v2.2)

The time-delay of the gravitationally lensed double quasar UM 673

T. A. Akhunov[1,3], R. W. Schmidt[2⋆], O. Burkhonov[1,3], E. R. Gaynullina[1], S. Gottlöber[4], K. Mirtadjieva[1,3], S. N. Nuritdinov[1,3], I. Tadjibaev[1,3], J. Wambsganss[2], L. Wisotzki[4], V. V. Bruevich[5], A. S. Gusev[5], A. Sergeyev[6], G. Smirnov[7]

1. Ulugh Beg Astronomical Institute of the Uzbek Academy of Sciences and Isaac Newton Institute of Chile, Uzbek Branch, Astronomicheskaya 33, Tashkent, 100052, Uzbekistan
2. Astronomisches Rechen-Institut, Zentrum für Astronomie der Universität Heidelberg, Mönchhofstraße 12-14, 69120 Heidelberg, Germany
3. National University of Uzbekistan, Physics Faculty, Tashkent, 100174, Uzbekistan
4. Astrophysikalisches Institut Potsdam, An der Sternwarte 16, 14482 Potsdam, Germany
5. Sternberg Astronomical Institute, Universitetski pr. 13, 119991, Moscow, Russia
6. Institute of Radio Astronomy of the National Academy of Sciences of Ukraine, Krasnoznamennaya 4, Kharkov, 61002, Ukraine
7. Astronomical Institute of Kharkov National University, 35 Sumskaya Ul., Kharkov, 61022, Ukraine

Version 20 February 2008

ABSTRACT

We present the results of a monitoring campaign of the gravitational double quasar UM 673 at Maydanak observatory from August 2001 to December 2006. We obtained light curves in the V-filter (101 nights) and the R-filter (208 nights), split up into five observing seasons. We find brightness variations and $V-R$ colour variations of the quasar on time scales of several years. The observing conditions at the telescope limited individual observing seasons to less than 150 days, which makes the estimation of the time-delay between the two lensed images by light curve correlation difficult. To overcome this problem we introduce a novel technique to measure the time-delay from the variation of the $V-R$ colour of the quasar, and use this to obtain a time-delay $\Delta t = (106.8\,\mathrm{days}\pm17.0)\,\mathrm{days}$ at 68 per cent confidence (image A leading).

Key words: cosmology: observations – gravitational lensing – quasars: individual: UM 673 (Q 0142-100)

1 INTRODUCTION

The quasar UM 673 = Q0142-100 ($z_\mathrm{q} = 2.719$) was discovered by MacAlpine & Feldman (1982) and was identified as a gravitational lens system by Surdej et al. (1987, 1988). The system consists of two quasar images (named A and B) that are lensed by an elliptical galaxy ($z_\mathrm{gal} = 0.49$). The angular separation between the images is 2.22 arcsec. Spectroscopic studies by Smette et al. (1992) showed the presence of well correlated $Ly\alpha$ lines in the spectra of both images. They concluded that the light bundles of both images pass through the same absorbing region (see also Miralda-Escudé & Rees 1993).

Irregular but continuous monitoring of UM 673 was carried out between 1987 and 1994 (Daulie et al. 1993; Courbin 1995; Borgeest & Schramm 1993; Lehar et al. 2000). Sinachopoulos et al. (2001) presented light curve data between 1995 and 2000 for the total magnitude of the system. They obtained 29 nights over 6 years of observations, detecting maximum variations of the quasar of $|\Delta m| \approx 0.26$ mag. Recently, Nakos et al. (2005) have presented the results of observations in Johnson V-filter and Gunn i-filter in the years 1998, 1999 and 2001 with some variability in both images at the level of 0.1 mag. In their light curve, Nakos et al. (2005) found a relation between the V-band brightness and the $V-i$ colour of image A. They suggest that this relation can be explained by microlensing. In 2002, Wisotzki et al. (2004) took spectra of both images of UM 673, but did not find any evidence for microlensing from their spectra. They showed that there is stronger dust extinction in the spectrum of image B than in image A, which can be explained by the proximity to the centre of the lensing galaxy.

We present a light curve of UM 673 with five seasons, allowing us to study the variability of UM 673 on short and long time-scales, and obtain the first measurement of the

⋆ E-mail: rschmidt@ari.uni-heidelberg.de

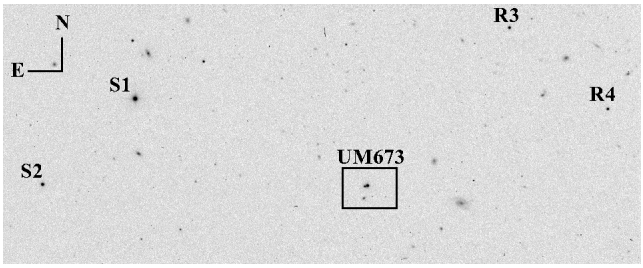

Figure 1. R-band image of the region around UM 673 obtained on August 26, 2003. The quasar images, the reference stars S2, R3 and R4, and the star S1 that we use for the PSF are labelled. The field is 8.2 arcmin×3.3 arcmin. The area marked with the box is shown in higher resolution in Fig. 2.

time-delay between the two gravitationally lensed images in this system.

2 OBSERVATIONS

We report in this paper on our photometric monitoring of UM 673. The observations were conducted in 2001 (August), 2003 (August 6 to November 18), 2004 (August 8 to December 5), 2005 (July 28 to January 23, 2006) and 2006 (August 15 to December 20) with the 1.5 m telescope AZT-22 at Maydanak observatory, South Uzbekistan (Artamonov et al. 1987; Ehgamberdiev et al. 2000). In the first season pilot observations were conducted. Starting in 2003 almost daily observations were carried out whenever weather permitted. The V and R-filters provide photometry in the Johnson-Cousins filters system. We observed on average four frames per night with an exposure time of 210 sec in V and 180 sec in R. The median seeing was 1.1 arcsec.

In total we obtained 101 nights in the V filter and 208 nights in the R filter. De-selecting poor seeing frames (more than 1.5 arcsec full-width at half maximum) and frames with high sky-background, we retained 69 nights in the V filter and 122 nights in the R filter. Up to 2005 the telescope was equipped with the BROCAM CCD detector (2000×800 pixels, pixel scale 0.26 arcsec). In time for the 2006 observing season a new detector with a larger field of view was installed (SNUCAM CCD, 4000×4000 pixels, pixel scale 0.26 arcsec). Bias correction and flat fielding of the images is done using standard IRAF software.

3 PHOTOMETRY

Photometry of the UM 673 images A and B is performed using the IRAF/DAOPHOT standard package (Stetson 1987), in a very similar way to Gaynullina et al. (2005). We use this method because it is well-suited to the mildly asymmetric and time-variable AZT-22 point spread function (PSF). The positions and magnitudes of both quasar images are fitted at the same time. Since image B is approximately 2 magnitudes fainter than image A, it is important to use low-background frames to obtain robust measurements.

Our field of view is shown in Fig. 1. Of the seven standard stars introduced for UM 673 by Sinachopoulos et al. (2001), the field includes their stars 3 and 4. To distinguish the star names from the other reference stars we call them R3 and R4. Since R3 and R4 are relatively faint (approximately 1 magnitude fainter than image A), we use the brighter star S2 for the relative flux calibration of the quasar images. Absolute flux calibration is then done with R3 by determining the magnitude difference S2 − R3 averaged over all seasons for each filter. With the published values by Sinachopoulos et al. (2001) ($m_{\mathrm{R,R3}} = 17.12 \pm 0.02$ mag, $(V-R)_{\mathrm{R3}} = 0.33 \pm 0.03$ mag), we obtain the following magnitudes for S2: $m_{R,\mathrm{S2}} = 16.21 \pm 0.04$ mag and $(V-R)_{S2} = 0.43 \pm 0.04$ mag.

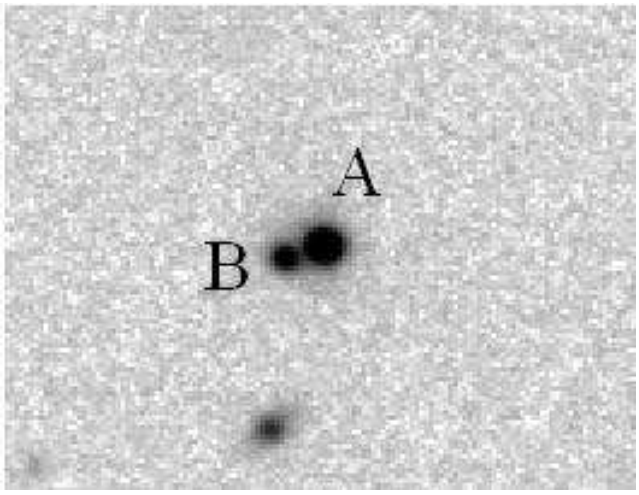

Figure 2. R-band zoom image of the central part of UM 673 (marked as a rectangle in Fig. 1). The field is 34 arcsec×26 arcsec. North is up and East is to the left. The foreground galaxy in the south does not affect our photometry. The lens galaxy ($m_{R,\mathrm{gal}} \approx 19.1$ mag, Surdej et al. 1988) is situated between the quasar images A and B and is too faint to be seen in this image.

To construct the point spread function we use the bright, but variable, star S1. We ignore the presence of the lensing galaxy near image B because it is too faint to be detected in our images ($m_{R,\mathrm{gal}} \approx 19.1$ mag, Surdej et al. 1988). As a consequence, a small fraction of the galaxy light is included in the quasar PSF fit, which may change the $V-R$ colour of image B slightly. The contribution is small, however, and does not affect the variability of the quasar image.

4 RESULTS

4.1 Light curves

We present the results of the V- and R-band photometry of UM 673 in Fig. 3 and Tables 2 and 3[1]. Our quoted error bars are the standard 1σ errors determined by DAOPHOT. Note that these error bars are likely underestimated due to systematic effects in the fitting process. The true uncertainty can be taken from the scatter of data points with small separations in time. In Fig. 3 the light curves of both quasar

[1] Tables 2 and 3 are available in the electronic version and at CDS.

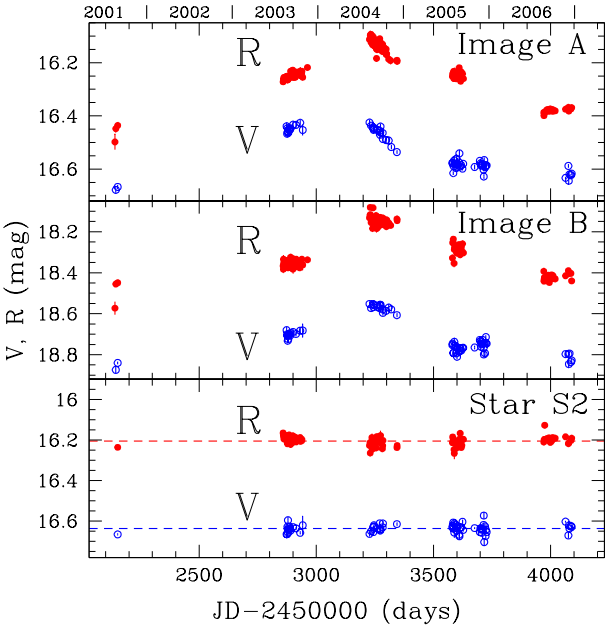

Figure 3. V-band and R-band light curves of UM 673 for images A (top panel) and B (middle panel). In the bottom panel the brightness of the reference star S2 is plotted whenever R3 was also observed to measure the relative brightness. The years corresponding to the Julian dates given at the bottom are indicated at the top.

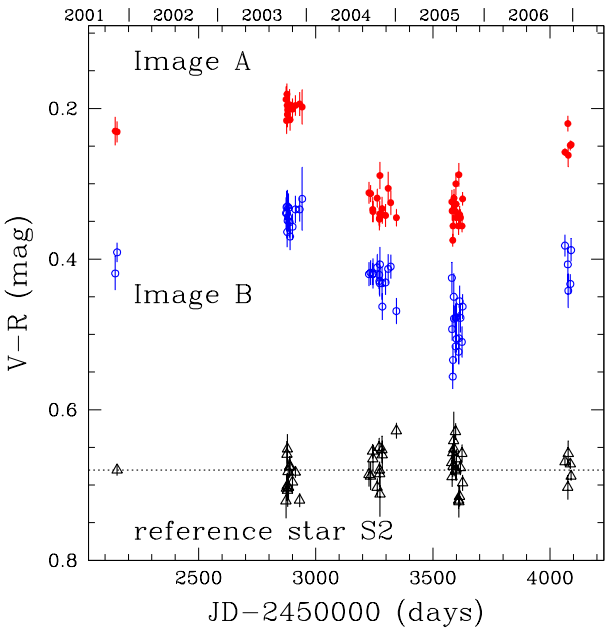

Figure 4. $V-R$ colour curve of UM 673 for the quasar images A (filled circles) and B (open circles). $V-R$ for the reference star S2 is plotted with open triangles whenever R3 was also observed to measure the colour. The average colour of the reference star $(V-R)_{S2} = 0.43$ mag is indicated with the dashed horizontal line (shifted by +0.25 mag for clarity).

images and the reference star S2 are plotted for both filters. We observe that both images of the quasar undergo a long-term variation with a time-scale of 1000 days or longer.

In Fig. 4 we show the $V-R$ colour curve for the quasar images and S2. The $V-R$ colour curve for both images undulates on time scales of several years. The colour difference of the reference star is consistent with being constant over the observed period. Note that the colour change is seen in both quasar images, shifted by the (to be determined) time-delay.

4.2 Time-delay measurement

Under the assumption that image A is leading and that microlensing does not significantly affect the light curves one can determine conservative limits on the time-delay by manually shifting the image B light curve with respect to image A.

To see this, consider Fig. 3 where we show both quasar image light curves. It can be seen from this plot that for $\Delta t < 70$ days, the 2003 and 2004 epochs cannot be accommodated with a single time-delay because the magnitude rise between these years is larger in image B than in image A. Above $\Delta t = 270$ days no agreement can be found between the light curve of image A in the interval 2003 to 2004 and the light curve of image B from 2004 to 2005, adjusted by the time-delay. Similar limits could be derived from the data for a leading image B, but we shall not pursue this here because the only viable lensing models require the quasar image further away from the lens centre to lead (e.g., Surdej et al. 1988).

However, the quasar light curve as measured in our data through either the V or the R band filters does not constrain the time-delay very well, because a large fraction of formally permitted time-delays are connected to little or no overlaps in the light curves of components A and B. Interpolation of the quasar light curve in these gaps cannot be done easily because quasars are known to vary unexpectedly.

The $V-R$ *colour curve* of quasars, on the other hand, is much less variable. We can assume that the colour curve is smooth in the light curve gaps. For a tighter limit on the time-delay, we thus turn to the remarkable $V-R$ colour changes of the quasar. We note in passing that there are not many lens systems known for which the brightness and the colour is observed to significantly vary; in the recent list of 10 known time-delays by Saha et al. (2006), only three systems have documented intrinsic colour variations: B0218+357 (Cohen et al. 2000, radio data), HE1104-1805 (Wisotzki et al. 1995) and HE 2149-2745 (Burud et al. 2002) (the latter showing rather small colour variations).

To determine the time-delay from the UM 673 colour light curve we employ the following strategy. We assume that the quasar colour changes are intrinsic to the quasars, and that they vary smoothly. We thus fit the colour curve *of both images* at the same time, shifted by the time-delay, with the Fourier series

$$(V-R)_{\rm model}(t) = a_0 + \sum_{k=1}^{n}\left(a_k \cos\frac{2\pi\, kt}{T_0} - b_k \sin\frac{2\pi\, kt}{T_0}\right) \quad (1)$$

($t = 0$ for Julian Date 2450000). For each observed data point in the colour curve, we calculate the sum

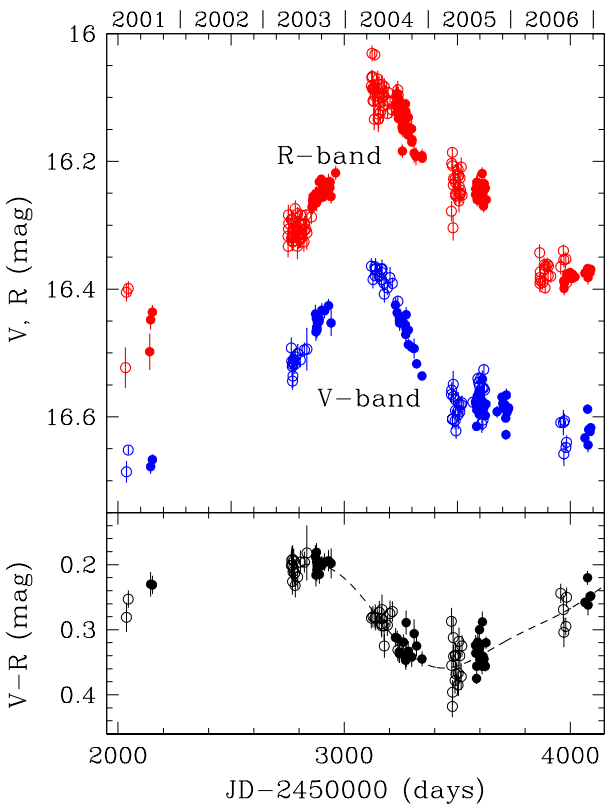

Figure 5. Top panel: Combined light curves of images A (filled circles) and B (open circles) of UM 673. Image B is shifted horizontally by the best-fitting time-delay $\Delta t = -106.8$ days and vertically by $\Delta m = 2.19$ mag in V-band and $\Delta m = 2.05$ mag in R-band. Julian dates at the bottom and years at the top are given at the respective epoch of image A. **Bottom panel:** $V-R$ colour curve for quasar images A and B, symbols as above. The colour curve for image B was shifted by the best-fitting time-delay and $\Delta(V-R) = -0.138$ mag. The dashed line is the best-fitting smooth interpolation function.

$$\chi^2 = \sum_{\text{data points i}} \frac{((V-R)_{\text{obs,i}} - (V-R)_{\text{model}})^2}{\sigma_{\text{i}}^2} \qquad (2)$$

where $(V-R)_{\text{obs,i}}$ are the observed $V-R$ values for images *A and* B, and σ_{i} are the corresponding measurement uncertainties. The best-fitting parameters correspond to the minimum of χ^2. Minimization is done with the Levenberg-Marquardt technique (Marquardt 1963).

The total number of free parameters in this model is $2n+4$ (Fourier coefficients, Fourier period T_0, time delay Δt and colour difference between the images $\Delta_{\text{V-R}} = (V-R)_{\text{A}} - (V-R)_{\text{B}}$). The degree n of the Fourier series is chosen by requiring that the F-test probability (Bevington & Robinson 1992) for a change from $n-1$ to n should be less than 5 per cent.

To avoid overly large gaps in the colour curve, we restrict ourselves to the 4 contiguous seasons from 2003 to 2006, which amounts to 50 days. We already find a robust solution for $n = 2$ and 8 free parameters. The number of degrees of freedom (d.o.f.) is $2\times 50 - 8 = 92$. Since the systematic scatter in the data is relatively large (χ^2/d.o.f. = 1.78), measurement uncertainties are estimated as described in Gaynullina et al. (2005) by repeating the above procedure for 10,000 Monte-Carlo realizations of the observed colour curves.

Table 1. Fourier coefficients with uncertainties for the best-fitting colour light curve described by eq. (1).

Parameter	
a_0	0.281 ± 0.006
a_1	-0.046 ± 0.032
b_1	-0.057 ± 0.025
a_2	-0.016 ± 0.011
b_2	-0.007 ± 0.021

Our result for the best-fitting time-delay in UM 673 is $\Delta t = 106.8 \pm 17.0$ days at 68 per cent confidence. The other fitted parameters are $T_0 = 1497.8 \pm 82.7$, $\Delta_{\text{V-R}} = 0.138 \pm 0.004$ mag. The results for the Fourier coefficients are listed in Table 1. In Fig. 5 (bottom panel) the variation of the $V-R$ colour with this time-delay can be seen together with the brightness variations of the quasar in V and R (top panel). The best-fitting smooth colour model is shown with a dashed line.

4.3 Testing the method

4.3.1 Simulated colour curves

We test our method by performing the time-delay estimation on simulated colour curves with pre-defined time-delays. For this we create 10,000 simulated colour curves with random Fourier coefficients and by varying the period T_0 by ± 20 per cent from the value found for the Maydanak data (Tab. 1). We introduce random time-delays between 90 and 120 days between the simulated colour curves of image A and B, and extract the simulated data points corresponding to the sampling of the observed colour curve (50 measurements). Since the result crucially depends on the size of the error bars and the amplitude of the variation, the simulated colour curves should have similar properties as the observed curve: we normalize the simulated curves to have a total amplitude Δ (V-R) = 0.15 mag and require a difference from the first to the last data point of less than 0.05 mag. The simulated curves also include Gaussian scatter according to the observed error bars.

For all 10,000 simulated colour curves time-delays are determined in the same way as it is done for the Maydanak observations. In Fig. 6 we show the distribution of the differences between the pre-defined and measured time-delays. We find that our method recovers the pre-defined time-delays within a root-mean-square uncertainty $\sigma = 19.5$ days at 68 per cent.

4.3.2 Application to a different system with known time-delay

As a further check on our method we carry out the same procedure with the 8 GHz and 15 GHz radio light curves of the gravitational lens B0218+357 published by Cohen et al. (2000). Data points are removed from this data set corresponding to the gaps between our 2003, 2004 and 2005

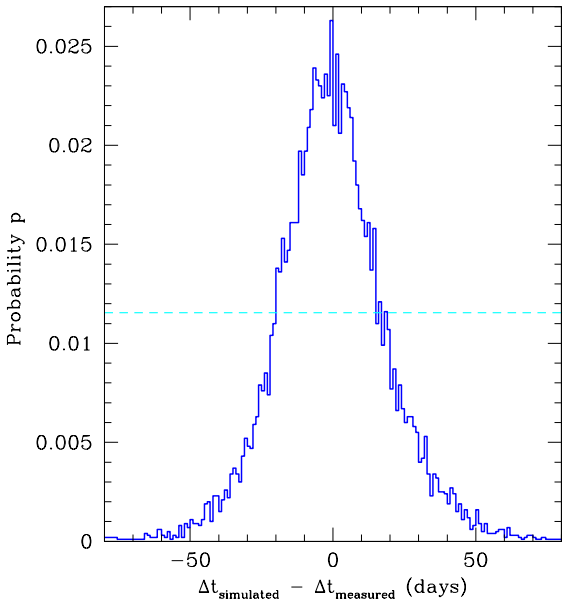

Figure 6. Histogram of the difference of pre-defined and measured time-delays Δt for 10,000 *simulated* colour curves. The intersections of the dashed lines and the histogram indicate the 68 per cent confidence interval.

data for UM 673. We cannot split the data set up into more seasons because the number of data points for each season would become too small. Since the Cohen et al. (2000) light curve is significantly shorter than our observing interval, ten days in the UM 673 light curve correspond to one day in the "hacked" B0218+357 light curve thus produced. The best-fitting time-delay obtained by Cohen et al. (2000) from their complete light curve was $\Delta t_{0218} = 10.1^{+1.5}_{-1.6}$. Carrying out our Fourier-series fitting of the colour curve (again up to $n = 2$) we find $\Delta t_{0218,\mathrm{hacked}} = 11.2 \pm 5.4$ days at 68 per cent confidence, which compares well with the published values for this system (Biggs et al. 1999; Cohen et al. 2000). The larger uncertainty can be attributed to the removal of data points.

5 SUMMARY AND CONCLUSIONS

We present V-filter and R-filter photometry of the gravitational lens system UM 673 taken at Maydanak Observatory (Uzbekistan) over the duration of 5.3 years between 2001 and 2006. We have observed brightness variations of the quasar with a maximum amplitude ≈ 0.4 mag and a time scale of the variations of several years.

Gaps in our light curve due to the observing conditions at the telescope make a determination of the time-delay based on the correlation of the light curves (e.g., Pelt et al. 1994, 1996) of images A and B rather difficult. Shifting the image B light curve manually with respect to the image A light curve yields conservative limits 70 days $< \Delta t <$ 270 days on the time-delay.

Importantly, we find that the $V - R$ colour light curve of the quasar is varying as well, but with a smaller amplitude. We use the colour light curve to determine the time-delay in UM 673 by assuming that the colour curve varies smoothly and modelling it with a low-order Fourier series. Using Monte-Carlo resampling of 50 measured $V - R$ data points we derive a time-delay $\Delta t = 106.8 \pm 17.0$ at 68 per cent confidence. Our method takes advantage of the fact that brightness variations of the quasar are accompanied by weaker variations of the colour. We have tested the method using simulated data, as well as data from another gravitational lens system (Cohen et al. 2000).

Lehar et al. (2000) have computed lens models for the lensing galaxy in UM 673. They determined the product of Hubble constant H_0 and the time-delay Δt predicted by their models. Our measurement of the time-delay implies $H_0 = 75 \pm 12$ km s^{-1}Mpc^{-1} for their singular isothermal ellipse (SIE) model, but for their constant mass-to-light ratio model (including external shear) it yields $H_0 = 107.7 \pm 18.3$ km s^{-1} Mpc^{-1}. Our time-delay measurement taken together with recent independent measurements of the Hubble constant (e.g., the Hubble key project result $H_0 = 72 \pm 8$ km s^{-1}Mpc^{-1}; Freedman et al. 2001) thus favours the singular isothermal ellipse model in this system.

We conclude by noting that with the measurement of the time-delay in UM 673, future efforts can now be directed at the microlensing effect in this system. The relatively short time-delay allows one to obtain intra-year difference light curves of ≈ 100 days duration if continuous monitoring is carried out. This should preferably be done with individual observing periods as long as possible (≈ 200 days).

ACKNOWLEDGMENTS

We thank B. P. Artamonov and V. N. Dudinov for useful advice on the realization of our observations. We thank the former German Ambassador to Uzbekistan, Dr. Martin Hecker, for his support of our collaboration. The Uzbek team thanks the ARI for hospitality during visits. This project was supported by the German Research Foundation (DFG), grant 436 USB 113/5/0-1. We also thank J. Fohlmeister and E. Koptelova for very useful comments. Observations for 2005 have been partially supported by the Science and Technology Center in the Ukraine (STCU), grant U127. This work was also partially supported by Russian Foundation for Basic Research (RFBR) grants 06-02-16857, 05-02-16454.

REFERENCES

Artamonov B.P., Novikov S.B., Ovchinnikov A.A., 1987, in: Methods for increasing the efficiency of optical telescopes, Gladyshev S.A. (eds.). Moscow: Moscow State Univ., p. 16

Bevington P. R., Robinson D. K., 1992, "Data reduction and error analysis for the physical sciences", WCB/McGraw-Hill, Boston

Biggs A.D., Browne I.W.A., Helbig P., Koopmans L.V.E., Wilkinson P.N., Perley R.A., 1999, MNRAS, 304, 349

Borgeest U., Schramm K.-J., 1993, in Proc. 1st Megaphot Workshop, pro public, Gronau, p. 105

Burud I., et al., 2002, A&A, 383, 71

Cohen A.S., Hewitt J.N., Moore C.B., Haarsma D.B., 2000, ApJ, 545, 578

Courbin F., 1995, Highlights Astron., 10, 659
Daulie G., Hainaut O., Hutsemékers D., et al., 1993, in 31st Liège Int. Astr. Col., Gravitational lenses in the Universe, p. 181
Ehgamberdiev S.A., Baijumanov A.K., Ilyasov S.P., et al., 2000, A&A Suppl. Ser., 145, 293
Fohlmeister J., et al., 2007, ApJ, 662, 62
Freedman W.L., et al., 2001, ApJ, 553, 47
Gaynullina E.R., Schmidt R.W., Akhunov T., et al., 2005, A&A 440, 53
Kochanek C.S., Morgan N.D., Falco E.E., McLeod B.A., Winn J.N., Dembicky J., Ketzeback B., 2006, ApJ, 640, 47
Lehár J., et al., 2000, ApJ, 536, 584
MacAlpine G.M., Feldman F.R., 1982, ApJ, 261, 412
Marquardt D.W., 1963, Journal of the Society for Industrial and Applied Mathematics, 11, 431
Miralda-Escudé J., Rees M.J., 1993, MNRAS, 260, 617
Nakos Th., Courbin F., Poels J., et al., 2005, A&A, 441, 443
Pelt J., Hoff W., Kayser R., Refsdal S., Schramm T., 1994, A&A, 286, 775
Pelt J., Kayser R., Refsdal S., Schramm T., 1996, A&A, 305, 97
Saha P., Coles J., Macciò A.V., Williams L.L.R., 2006, ApJL, 650, L17
Sinachopoulos D., Nakos Th., Boumis P., et al., 2001, AJ, 122, 1692
Smette A., Surdej J., Shaver P.A., et al., 1992, ApJ, 389, 39
Stetson P., 1987, PASP 99, 191
Surdej J., Swings J.-P., Magain P., et al., 1987, Nature, 329, 695
Surdej J., Magain P., Swings J.-P., et al., 1988, A&A, 198, 49
Vuissoz C., et al., 2007, A&A, 464, 845
Wisotzki L., Koehler T., Ikonomou M., Reimers D., 1995, A&A, 297, L59
Wisotzki L., Becker T., Christensen L., et al., 2004, Astron. Nachr., 325, 135

This paper has been typeset from a TEX/ LATEX file prepared by the author.

Table 2. *V*-band photometry of UM 673. In this table the Julian Dates (JD) and the magnitudes for image A (column 2) and image B (column 3) are listed.

JD-2450000	$m_{\rm A}$	$m_{\rm B}$
2144	16.678 ± 0.011	18.874 ± 0.017
2152	16.667 ± 0.008	18.840 ± 0.006
2873	16.439 ± 0.014	18.680 ± 0.017
2875	16.467 ± 0.014	18.701 ± 0.016
2877	16.446 ± 0.011	18.709 ± 0.015
2878	16.460 ± 0.011	18.732 ± 0.013
2879	16.460 ± 0.011	18.706 ± 0.017
2880	16.464 ± 0.013	18.724 ± 0.018
2882	16.452 ± 0.011	18.703 ± 0.015
2884	16.450 ± 0.011	18.698 ± 0.015
2888	16.451 ± 0.015	18.706 ± 0.015
2890	16.447 ± 0.012	18.694 ± 0.013
2901	16.433 ± 0.011	18.689 ± 0.014
2913	16.434 ± 0.011	18.699 ± 0.011
2931	16.426 ± 0.010	18.683 ± 0.011
2942	16.453 ± 0.020	18.682 ± 0.033
3227	16.425 ± 0.011	18.552 ± 0.013
3234	16.437 ± 0.009	18.573 ± 0.014
3243	16.443 ± 0.009	18.553 ± 0.008
3244	16.449 ± 0.009	18.567 ± 0.008
3245	16.453 ± 0.012	18.557 ± 0.012
3246	16.446 ± 0.015	18.556 ± 0.016
3262	16.453 ± 0.007	18.568 ± 0.009
3271	16.456 ± 0.005	18.557 ± 0.009
3272	16.471 ± 0.010	18.573 ± 0.011
3273	16.462 ± 0.009	18.562 ± 0.010
3274	16.440 ± 0.011	18.556 ± 0.014
3283	16.464 ± 0.011	18.579 ± 0.013
3284	16.487 ± 0.009	18.596 ± 0.013
3298	16.491 ± 0.009	18.586 ± 0.011
3309	16.493 ± 0.016	18.570 ± 0.017
3320	16.517 ± 0.007	18.579 ± 0.009
3344	16.536 ± 0.006	18.607 ± 0.009
3581	16.576 ± 0.012	18.753 ± 0.013
3582	16.579 ± 0.009	18.746 ± 0.012
3585	16.615 ± 0.007	18.792 ± 0.015
3586	16.589 ± 0.009	18.791 ± 0.015
3589	16.567 ± 0.014	18.737 ± 0.021
3590	16.579 ± 0.011	18.756 ± 0.011
3597	16.596 ± 0.006	18.794 ± 0.014
3598	16.561 ± 0.010	18.761 ± 0.011
3599	16.580 ± 0.008	18.778 ± 0.013
3601	16.591 ± 0.009	18.810 ± 0.012
3610	16.575 ± 0.007	18.785 ± 0.011
3611	16.541 ± 0.014	18.778 ± 0.029
3614	16.590 ± 0.006	18.768 ± 0.012
3618	16.585 ± 0.009	18.780 ± 0.011
3624	16.598 ± 0.006	18.769 ± 0.014
3627	16.580 ± 0.005	18.766 ± 0.011
3676	16.592 ± 0.009	18.765 ± 0.009
3698	16.569 ± 0.005	18.728 ± 0.009
3701	16.579 ± 0.004	18.734 ± 0.007
3703	16.586 ± 0.004	18.761 ± 0.009
3705	16.584 ± 0.004	18.740 ± 0.007
3706	16.583 ± 0.014	18.749 ± 0.014
3710	16.581 ± 0.007	18.728 ± 0.005
3714	16.602 ± 0.006	18.767 ± 0.011

Table 2. (continued)

JD-2450000	$m_{\rm A}$	$m_{\rm B}$
3715	16.628 ± 0.008	18.799 ± 0.014
3717	16.566 ± 0.010	18.743 ± 0.017
3720	16.593 ± 0.007	18.793 ± 0.016
3723	16.589 ± 0.006	18.743 ± 0.014
3724	16.588 ± 0.005	18.714 ± 0.008
3727	16.586 ± 0.005	18.746 ± 0.010
4064	16.633 ± 0.004	18.797 ± 0.008
4076	16.588 ± 0.007	18.797 ± 0.020
4078	16.644 ± 0.012	18.846 ± 0.019
4081	16.620 ± 0.004	18.794 ± 0.011
4087	16.623 ± 0.004	18.836 ± 0.008
4090	16.617 ± 0.004	18.828 ± 0.011

Table 3. *R*-band photometry of UM 673. In this table the Julian Dates (JD) and the magnitudes for image A (column 2) and image B (column 3) are listed.

JD-2450000	$m_{\rm A}$	$m_{\rm B}$
2140	16.498 ± 0.029	18.573 ± 0.032
2144	16.448 ± 0.015	18.455 ± 0.014
2152	16.436 ± 0.011	18.449 ± 0.011
2858	16.272 ± 0.009	18.367 ± 0.013
2859	16.270 ± 0.012	18.383 ± 0.017
2860	16.261 ± 0.007	18.334 ± 0.016
2861	16.268 ± 0.013	18.356 ± 0.017
2862	16.255 ± 0.009	18.347 ± 0.013
2873	16.251 ± 0.010	18.341 ± 0.013
2875	16.251 ± 0.010	18.370 ± 0.014
2876	16.256 ± 0.008	18.341 ± 0.016
2877	16.265 ± 0.009	18.370 ± 0.019
2878	16.264 ± 0.014	18.368 ± 0.015
2879	16.252 ± 0.013	18.376 ± 0.015
2880	16.262 ± 0.009	18.375 ± 0.013
2882	16.256 ± 0.007	18.359 ± 0.012
2883	16.256 ± 0.009	18.368 ± 0.014
2884	16.253 ± 0.010	18.366 ± 0.011
2888	16.256 ± 0.015	18.355 ± 0.014
2889	16.250 ± 0.012	18.347 ± 0.012
2890	16.232 ± 0.008	18.324 ± 0.013
2898	16.245 ± 0.005	18.357 ± 0.014
2899	16.228 ± 0.006	18.352 ± 0.017
2900	16.254 ± 0.010	18.383 ± 0.020
2901	16.232 ± 0.009	18.332 ± 0.011
2902	16.248 ± 0.011	18.357 ± 0.012
2903	16.249 ± 0.014	18.365 ± 0.016
2904	16.242 ± 0.004	18.345 ± 0.010
2905	16.256 ± 0.006	18.371 ± 0.016
2907	16.248 ± 0.006	18.366 ± 0.015
2910	16.255 ± 0.006	18.349 ± 0.017
2911	16.240 ± 0.009	18.370 ± 0.015
2912	16.239 ± 0.006	18.371 ± 0.014
2913	16.238 ± 0.007	18.365 ± 0.014
2914	16.235 ± 0.006	18.334 ± 0.008
2915	16.245 ± 0.010	18.371 ± 0.014
2929	16.236 ± 0.010	18.376 ± 0.015
2930	16.248 ± 0.013	18.358 ± 0.012
2931	16.232 ± 0.012	18.349 ± 0.011
2932	16.234 ± 0.008	18.348 ± 0.012
2937	16.241 ± 0.006	18.356 ± 0.016
2938	16.232 ± 0.008	18.334 ± 0.009
2942	16.255 ± 0.011	18.362 ± 0.026
2962	16.218 ± 0.010	18.337 ± 0.011
3227	16.113 ± 0.010	18.132 ± 0.010
3229	16.112 ± 0.009	18.119 ± 0.012
3230	16.097 ± 0.017	18.081 ± 0.013
3231	16.109 ± 0.009	18.117 ± 0.009
3232	16.094 ± 0.011	18.136 ± 0.014
3234	16.124 ± 0.007	18.155 ± 0.009
3235	16.095 ± 0.011	18.137 ± 0.015
3237	16.116 ± 0.016	18.136 ± 0.014
3238	16.112 ± 0.012	18.156 ± 0.017
3240	16.133 ± 0.015	18.184 ± 0.017
3241	16.124 ± 0.009	18.136 ± 0.014
3242	16.102 ± 0.007	18.083 ± 0.009
3243	16.109 ± 0.013	18.133 ± 0.012
3244	16.112 ± 0.011	18.148 ± 0.018
3255	16.114 ± 0.008	18.121 ± 0.013
3256	16.146 ± 0.009	18.147 ± 0.012

Table 3. (continued)

JD-2450000	$m_{\rm A}$	$m_{\rm B}$
3257	16.184 ± 0.010	18.184 ± 0.020
3258	16.148 ± 0.011	18.176 ± 0.013
3259	16.151 ± 0.011	18.183 ± 0.015
3261	16.141 ± 0.005	18.129 ± 0.013
3262	16.134 ± 0.010	18.157 ± 0.015
3267	16.147 ± 0.016	18.173 ± 0.017
3271	16.110 ± 0.008	18.136 ± 0.016
3272	16.124 ± 0.010	18.144 ± 0.014
3273	16.122 ± 0.014	18.130 ± 0.014
3274	16.151 ± 0.014	18.149 ± 0.018
3282	16.158 ± 0.009	18.163 ± 0.019
3283	16.131 ± 0.011	18.147 ± 0.018
3284	16.146 ± 0.008	18.133 ± 0.013
3298	16.149 ± 0.012	18.155 ± 0.012
3299	16.170 ± 0.005	18.175 ± 0.008
3300	16.166 ± 0.008	18.142 ± 0.009
3309	16.187 ± 0.015	18.157 ± 0.011
3317	16.192 ± 0.014	18.169 ± 0.012
3344	16.191 ± 0.009	18.138 ± 0.014
3345	16.195 ± 0.006	18.146 ± 0.012
3581	16.252 ± 0.010	18.328 ± 0.016
3582	16.243 ± 0.009	18.253 ± 0.009
3585	16.240 ± 0.004	18.236 ± 0.008
3586	16.233 ± 0.011	18.257 ± 0.011
3588	16.260 ± 0.010	18.354 ± 0.020
3589	16.233 ± 0.015	18.287 ± 0.023
3590	16.260 ± 0.005	18.277 ± 0.013
3597	16.259 ± 0.006	18.278 ± 0.015
3598	16.261 ± 0.011	18.283 ± 0.016
3599	16.253 ± 0.007	18.301 ± 0.013
3600	16.246 ± 0.010	18.304 ± 0.013
3610	16.219 ± 0.009	18.262 ± 0.011
3611	16.253 ± 0.008	18.273 ± 0.019
3613	16.235 ± 0.005	18.272 ± 0.014
3614	16.249 ± 0.010	18.312 ± 0.017
3615	16.237 ± 0.009	18.289 ± 0.015
3616	16.270 ± 0.009	18.300 ± 0.016
3618	16.240 ± 0.007	18.302 ± 0.016
3619	16.235 ± 0.013	18.276 ± 0.015
3620	16.244 ± 0.008	18.300 ± 0.012
3621	16.241 ± 0.007	18.295 ± 0.013
3624	16.242 ± 0.005	18.259 ± 0.015
3628	16.260 ± 0.008	18.303 ± 0.012
3971	16.387 ± 0.005	18.393 ± 0.013
3972	16.399 ± 0.010	18.441 ± 0.014
3973	16.391 ± 0.004	18.432 ± 0.014
3974	16.387 ± 0.004	18.423 ± 0.013
3975	16.387 ± 0.004	18.437 ± 0.010
3984	16.377 ± 0.004	18.440 ± 0.011
3991	16.376 ± 0.006	18.412 ± 0.011
3993	16.383 ± 0.005	18.419 ± 0.012
3995	16.380 ± 0.004	18.448 ± 0.009
3999	16.374 ± 0.004	18.414 ± 0.010
4005	16.377 ± 0.003	18.411 ± 0.010
4009	16.383 ± 0.006	18.429 ± 0.012
4010	16.377 ± 0.004	18.414 ± 0.008
4020	16.381 ± 0.004	18.430 ± 0.010
4064	16.375 ± 0.003	18.415 ± 0.012
4076	16.368 ± 0.008	18.390 ± 0.009
4078	16.382 ± 0.010	18.404 ± 0.012
4087	16.374 ± 0.005	18.403 ± 0.010
4090	16.369 ± 0.002	18.440 ± 0.010